International Journal of Civil Engineering

Structure
Concrete

# A model for prediction of compressive strength of chemically activated high phosphorous slag content cement

**A. Allahverdi[1,*], M. Mahinroosta[1]**

Received: May 2013, Accepted: January 2014

***Abstract***

*It was found out that the logarithmic models fit the cement–slag blend systems well. In the present study, based on the experimental results, a logarithmic model has been developed to predict the compressive strength of chemically activated high phosphorous slag content cement. Mixes of phosphorous slag (80 wt.%), Portland cement (14 wt.%) and compound chemical activator (6 wt.%) were prepared at different Blaine finenesses using a laboratory ball mill. Compressive strengths of mortar specimens cured in lime-saturated water were measured at different curing times. Mathematical model was prepared in terms of curing time and water-to-cement ratio as independent variables and compressive strength as dependent variable. The comparisons between the model reproductions and the experimentally obtained results confirm the applicability of the presented model.*

***Keywords:*** *Phosphorous slag, Compressive strength, Water-to-cement ratio, Modeling.*

## 1. Introduction

Phosphorous slag (PHS) is an industrial by-product of yellow phosphor production via electric furnace method, in which calcium oxide (CaO) and silicon dioxide ($SiO_2$) account for over 80% [1, 2]. The minor components in PHS, which depend on the nature of phosphate ores used, are 2.5%-5% $Al_2O_3$, 0.2%-2.5% $Fe_2O_3$, 0.5%-3.0% MgO, 1%-5% $P_2O_5$, and 0-2.5% F. PHS exhibits latent cementing properties and can be considered as a supplementary cementing material but it is less reactive than blast furnace slag [1, 3].

Nonetheless, with using PHS at high replacement levels, the poor early-age strength of Portland cement was resulted [4] and therefore, it is essential to use an auxiliary activation technique such as thermal curing, chemical activation, and mechanical activation for reactivity improvement [4-6]. In the present study, chemically activated high phosphorous slag content cement (CAPHSC in short) was mechanically activated using a laboratory ball mill for the purpose of compressive strength improvement. CAPHSC is a high PHS content cement that is chemically activated using a Portland cement-based compound chemical activator. This activator was introduced in the some recent studies [7-10] and it contains a mixture of different solid chemical activators including anhydrite and sodium sulphate.

Compressive strength is the most important property for quality control purpose in cement industry. It is time-consuming way to wait for getting experimental compressive strength data, therefore, rapid estimation of compressive strength has attracted interests of many researches [11-21]. One of the common methods for quick determination of compressive strength is to apply mathematical models [11, 12]. Many modeling methods have been used to predict the properties (compressive strength in particular) of heterogeneous systems such as cementing materials, including artificial neural network [13-16] and analytical model (e.g., regression) [17-21]. These methods lead to models with insufficient accuracy, so that they are considered as engineering approximations [22]. The experimental data-based models are often simple and they take into account the effects of parameters such as curing time, water-to-cement ratio, curing temperature, and Blaine fineness of cement [23, 24]. But, there is no comprehensive model to consider the effects of all these factors properly [24]. Over the past decades up to now, application of analytical models such as regression for taking into account these factors has been a common approach [18-21]. Linear regression is a common method to show the dependence between a dependent variable and two or more independent variables [19].

Among above-mentioned factors, the water-to-cement ratio is a basic one in paste and mortar proportioning. This factor has an important effect on the characteristics (such as compressive strength) of mortars and concrete [25]. The aim of this paper is to present a mathematical model for prediction of compressive strength of CAPHSC mortar.

** Corresponding author: ali.allahverdi@iust.ac.ir*
*1 Cement Research Center, School of Chemical Engineering, Iran University of Science and Technology, Narmak 1684613114, Tehran, Iran*

The modeling was performed using a developed regression analysis based on experimental results.

## 2. Materials and Methods

### *2.1. Materials*

#### *2.1.1. Phosphorous slag*

Granulated PHS was supplied from a phosphoric acid plant located in south east of Tehran, Iran. Its chemical oxide composition determined according to ASTM standard C311 is given in Table 1.

**Table 1** Chemical composition of granulated phosphorous slag (in wt.%)

| $SiO_2$ | $Al_2O_3$ | $Fe_2O_3$ | CaO | MgO | $P_2O_5$ | $K_2O$ | $Na_2O$ | LOI |
|---|---|---|---|---|---|---|---|---|
| 38.42 | 7.65 | 0.90 | 45.14 | 2.60 | 1.50 | 0.56 | 0.43 | 1.87 |

Results confirm the relative quality of the material due to its relatively high silicon dioxide and calcium oxide contents according to ASTM standard C618. The X-ray diffraction pattern of PHS was shown in Fig. 1. The only observed phase was periclase (MgO) . The density of PHS was determined according to ASTM standard C188 and it was 2940 kg/m$^3$.

#### *2.1.2. Portland cement*

The cement used was ASTM Type II Portland cement (PC). Its density and Blaine specific surface area were 3120 kg/m$^3$ and 302 m$^2$/kg, respectively. The chemical composition and Bouge's potential phase composition of this cement are given in Table 2 and Table 3, respectively.

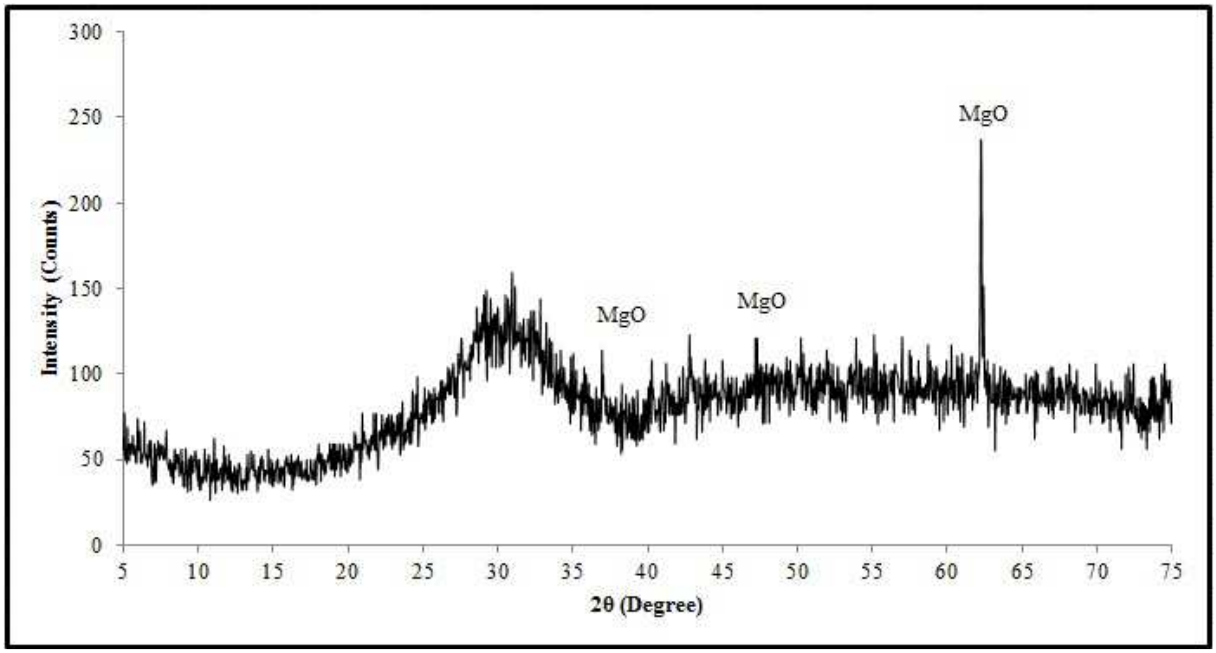


**Fig. 1** X-ray diffraction pattern of phosphorous slag

**Table 2** Chemical composition of PC (in wt.%)

| $SiO_2$ | $Al_2O_3$ | $Fe_2O_3$ | CaO | MgO | $K_2O$ | $Na_2O$ | $SO_3$ | LOI | free CaO |
|---|---|---|---|---|---|---|---|---|---|
| 22.50 | 4.15 | 3.44 | 63.26 | 3.25 | 0.65 | 0.20 | 1.80 | 0.61 | 0.72 |

**Table 3** Bouge's potential phase composition of PC (in wt.%)

| $C_3S$ | $C_2S$ | $C_3A$ | $C_4AF$ |
|---|---|---|---|
| 45.62 | 30.16 | 5.18 | 10.47 |

C = CaO, S = $SiO_2$, A = $Al_2O_3$, F = $Fe_2O_3$

#### *2.1.3. Compound activator*

Choosing of the compound chemical activator was done according to the some recent researches [7-10]. It contains $Na_2SO_4$ (2 wt.%) and anhydrite (4 wt.%). Sodium sulphate was purchased from Merck. The chemical composition of anhydrite (in wt.%) was as follows: CaO-36.00, $SO_3$-54.38, and $SiO_2$-5.88.

*2.2. Methods*

*2.2.1. Grinding*

Batch grinding tests were performed in a laboratory ball mill with the length and diameter of 0.30 and 0.26 m, respectively. At the beginning, inter-grinding of PHS (80 wt.%), PC (14 wt.%) and compound chemical activator (6 wt.%) was done until they reached the desired Blaine fineness levels, namely 205, 250, 303, 351, 400, and 450 $m^2$/kg.

*2.2.2. Blaine fineness*

The values of Blaine specific surface area were determined according to ASTM standard C204 using Blaine air-permeability apparatus.

*2.2.3. Water-to-cement ratio*

Water-to-cement ratios for paste and mortar of each Blaine fineness were determined using flow table test according to ASTM standard C230. The water-to-cement ratios of pastes and mortars can be determined if the normal consistency is known. In order to have normal consistency for each paste and mortar mix, control flow table tests were performed. For these tests, PC mortar and paste of normal consistency were used as reference. Water-to-cement ratio for PC paste and mortar were 0.27 and 0.485, respectively.

*2.2.4. Compressive strength*

AZMOONTEST test machine was used to determine the 7-, 14-, 28-, 90-, and 180-day compressive strengths of CAPHSC mortar specimens. Three specimens were used for each measurement and the average of the three values was reported as the result.

*2.2.5. Preparation of specimens*

For each Blaine fineness, enough mortar specimens of the size 5×5×5 $cm^3$ were prepared in accordance with ASTM standard C109. After casting, the molds were stored at an atmosphere of more than 95% relative humidity at 25 ºC for the first 24 h and then after demolding, the specimens were cured in lime-saturated water at 25 ºC until the time of testing.

## 3. Model Formulation

The results of compressive strength for all Blaine finenesses used in this study, are given in Table 4.

At first, the best curve fitting was done using data from Table 4. Investigating the variations of compressive strength versus curing age of specimens shows that the best curve fitting for all Blaine finenesses is a logarithmic relationship as: $R=\alpha Ln(t)+\beta$; where R and t are the compressive strength and curing time in MPa and days, respectively. The curves associated with different Blaine finenesses have their own distinct α and β. The purpose of this study is to prepare a comprehensive model with the same α and β for all Blaine finenesses.

**Table 4** Experimental compressive strengths of CAPHSC mortar specimens

| Blaine fineness ($m^2$/kg) | Compressive strength (MPa) | | | | |
|---|---|---|---|---|---|
| | 7 days | 14 days | 28 days | 90 days | 180 days |
| 205 | 14.32 | 27.73 | 39.32 | 58.93 | 72.84 |
| 250 | 21.92 | 34.41 | 46.90 | 67.33 | 81.53 |
| 303 | 33.32 | 45.81 | 58.30 | 79.34 | 91.83 |
| 351 | 44.77 | 57.26 | 69.75 | 90.79 | 101.53 |
| 400 | 56.28 | 68.77 | 81.40 | 102.30 | 114.80 |
| 450 | 67.38 | 79.87 | 92.93 | 113.40 | 125.89 |

*3.1. Variables of model*

For prediction of the compressive strength of CAPHSC mortars, curing time (t) and water-to-cement ratio (λ) are considered as independent variables and the compressive strength (R) as dependent variable of the model. The effect of Blaine fineness on the compressive strength is taken into account by means of the water-to-cement ratio variable, λ. In other words, water-to-cement ratio is an equivalent for considering Blaine fineness.

*3.2. Dimensionless variables*

It is here provided dimensionless insight into model. μ in Eq. (1) is as dimensionless age of curing that is calculated from division of curing time (t) by $t_p$. At first, values of 7, 14, and 28 days were assigned to $t_p$. Later investigations using curve fitting showed that values of 7 and 14 were not proper values for $t_p$, because plotted curves didnot have high correlation factors. By choosing the value of 28 days for $t_p$, the correlation factors of the curves were high and they were about 0.99.

$$\mu = t/t_p \quad (1)$$

θ in Eq. (2) is as dimensionless water-to-cement ratio:

$$\theta = \lambda/(\lambda_p-\lambda) \quad (2)$$

in which $\lambda_p$ is water-to-cement ratio of PC mortar and its value is 0.485. The values of θ are given in Table 5.

σ is known as dimensionless compressive strength and its value is calculated from Eq. (3):

$$\sigma = R/R_p \quad (3)$$

in which $R_p$ is equals 42.5 MPa. Inasmuch as the value of 28 days was considered for $t_p$, the 28-day compressive strength of PC (42.5 MPa) was attributed to $R_p$ for better dependence between curing time and compressive strength. The values of determined σ for all Blaine finenesses are given in Tables (6) and (7).

**Table 5** Values of θ for all Blaine finenesses

| Blaine fineness ($m^2$/kg) | λ | θ |
|---|---|---|
| **205** | 0.360 | 2.880 |
| **250** | 0.364 | 3.010 |
| **303** | 0.370 | 3.217 |
| **351** | 0.376 | 3.450 |
| **400** | 0.382 | 3.710 |
| **450** | 0.388 | 3.900 |

**Table 6** Dimensionless values for Blaine finenesses of 205, 250, and 303 $m^2$/kg

| t | μ | 205 $m^2$/kg | | | 250 $m^2$/kg | | | 303 $m^2$/kg | | |
|---|---|---|---|---|---|---|---|---|---|---|
| | | θ.μ | R | σ | θ.μ | R | σ | θ.μ | R | σ |
| **7** | 0.25 | 0.72 | 14.32 | 0.3369 | 0.75 | 21.92 | 0.5158 | 0.80 | 33.32 | 0.7840 |
| **14** | 0.50 | 1.44 | 27.73 | 0.6525 | 1.51 | 34.41 | 0.8096 | 1.61 | 45.81 | 1.0779 |
| **28** | 1.00 | 2.88 | 39.32 | 0.9252 | 3.01 | 46.90 | 1.1035 | 3.22 | 58.30 | 1.3717 |
| **90** | 3.21 | 9.26 | 58.93 | 1.3866 | 9.68 | 67.33 | 1.5842 | 10.34 | 79.34 | 1.8668 |
| **180** | 6.43 | 18.51 | 72.84 | 1.7139 | 19.35 | 81.53 | 1.9183 | 20.68 | 91.83 | 2.1607 |

**Table 7** Dimensionless values for Blaine finenesses of 351, 400, and 450 $m^2$/kg

| t | μ | 351 $m^2$/kg | | | 400 $m^2$/kg | | | 450 $m^2$/kg | | |
|---|---|---|---|---|---|---|---|---|---|---|
| | | θ.μ | R | σ | θ.μ | R | σ | θ.μ | R | σ |
| **7** | 0.25 | 0.86 | 44.77 | 1.0534 | 0.93 | 56.28 | 1.3365 | 0.98 | 67.38 | 1.5854 |
| **14** | 0.50 | 1.72 | 57.26 | 1.3473 | 1.86 | 68.77 | 1.6181 | 1.95 | 79.87 | 1.8793 |
| **28** | 1.00 | 3.45 | 69.75 | 1.6412 | 3.71 | 81.40 | 1.9153 | 3.90 | 92.93 | 2.1866 |
| **90** | 3.21 | 11.09 | 90.79 | 2.1362 | 11.92 | 102.30 | 2.4070 | 12.54 | 113.40 | 2.6682 |
| **180** | 6.43 | 22.18 | 101.53 | 2.3889 | 23.85 | 114.80 | 2.7012 | 25.07 | 125.89 | 2.9621 |

*3.3. Parameters of model*

In order to obtain the parameters of the model, the values of σ versus μ.θ at all Blaine finenesses are plotted. Fig. 2 illustrates this curve fitting. In this way, the values of α and β related to each Blaine fineness are obtained. They are given in Table 8. A regression analysis is then performed to have an idea about the parameters. For statistical analyses, linear regression analysis (LRA) was employed. LRA generally requires a strong correlation between the independent and dependent variables. The purpose of LRA is to simultaneously indentify one or more independent variables that explain variations in the dependent variable.

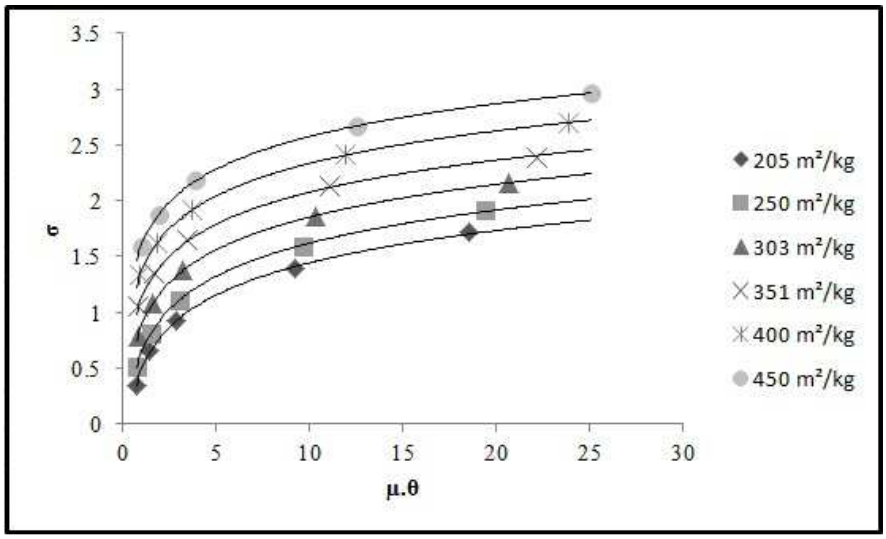


**Fig. 2** Values of σ versus μ.θ for all Blaine finenesses used in this study

**Table 8** Values of α and β for all Blaine finenesses

| Blaine fineness ($m^2$/kg) | α | β |
|---|---|---|
| **205** | 0.4167 | 0.4831 |
| **250** | 0.4280 | 0.6335 |
| **303** | 0.4240 | 0.8765 |
| **351** | 0.4142 | 1.1218 |
| **400** | 0.4240 | 1.3568 |
| **450** | 0.4236 | 1.5994 |

$$Y = a + b_1X_1 + b_2X_2 + \ldots b_kX_k \pm e, \quad (4)$$

Where Y is the dependent variable; a is the Y-intercept; $b_1$, $b_2$, and $b_k$ are the slopes related to $X_1$, $X_2$, and $X_k$, respectively; $X_1$, $X_2$, and $X_k$ are the values of the independent variables; and e represents the error.

It can be seen from Table 8 that values of α are close together. Therefore, the average of values of α was calculated and it was considered as constant parameter of the model. $\bar{\alpha}$ represents this constant parameter. LRA was then used to correlate the values of β with water-to-cement ratio. In other words, the values of β were considered as a linear function of water-to-cement ratio (λ). Resulted function in Eq. (5) is the second parameter of model, which is known as $\bar{\beta}$:

$$\bar{\beta} = 39.7282(\lambda)-13.8218 \quad (5)$$

Finally, the model for prediction of the compressive strength of CAPHSC mortar is as follows:

$$\sigma = \bar{\alpha}\ln(\theta.\mu) + \bar{\beta} \quad (6)$$

In which
$\sigma = R/42.50$
$\bar{\alpha} = 0.4218$
$\mu = t/28$
$\theta = \lambda/(0.485-\lambda)$
$\bar{\beta} = 39.7282(\lambda)-13.8218$

## 4. Model Verification

Aiming at a quantitative test of the predictive capability of the presented strength model for CAPHSC mortar, model predictions with experimental data are now compared. The predicted values have been plotted against their respective experimentally obtained values in Fig. 3 for all Blaine finenesses. It can be seen from this figure that there is a good correlation between experimental values and those predicted from the model. Also, comparison of experimental and predicted values of the 270-day compressive strength of CAPHSC mortar at Blaine finenesses of 303, 351, 400, and 450 $m^2$/kg is shown in Fig. 4. It is obvious from Figs. 3 and 4 that there is a good agreement between the experimental data and prediction of the mathematical model.

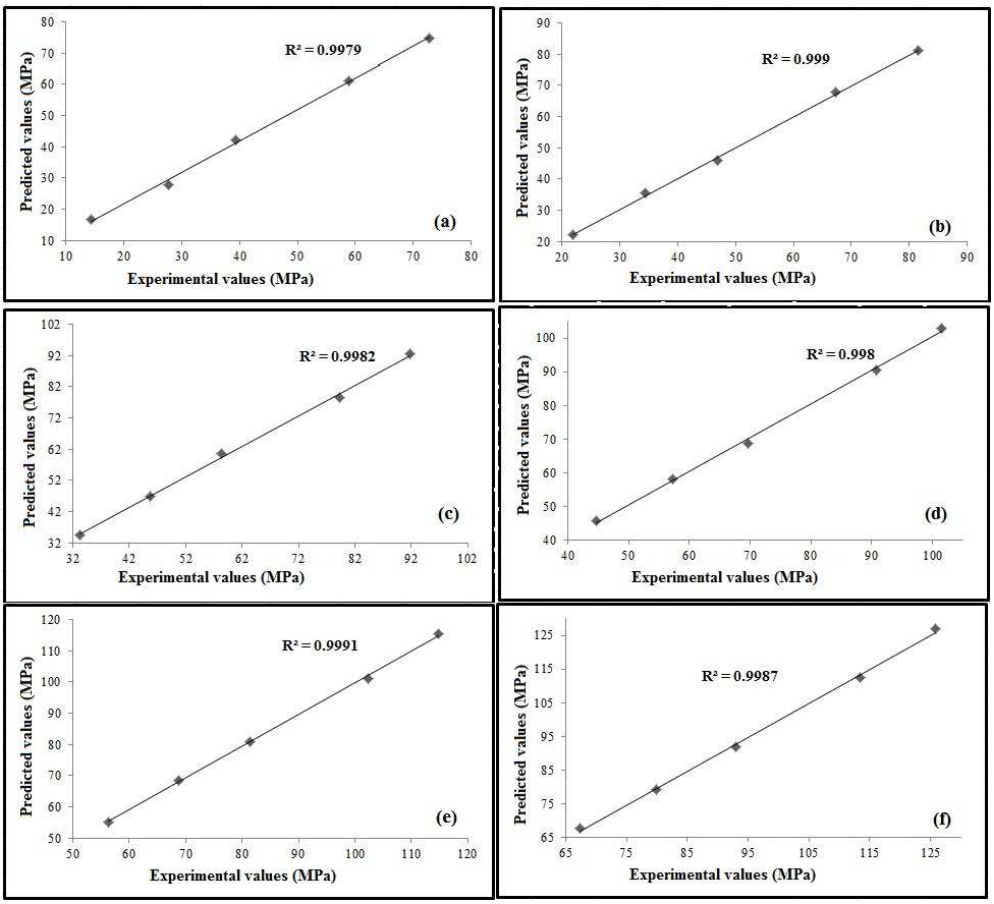


**Fig. 3** Predicted and experimental compressive strengths of CAPHSC mortar for Blaine finenesses of (a) 205, (b) 250, (c) 303, (d) 351, (e) 400, and (f) 450 $m^2$/kg

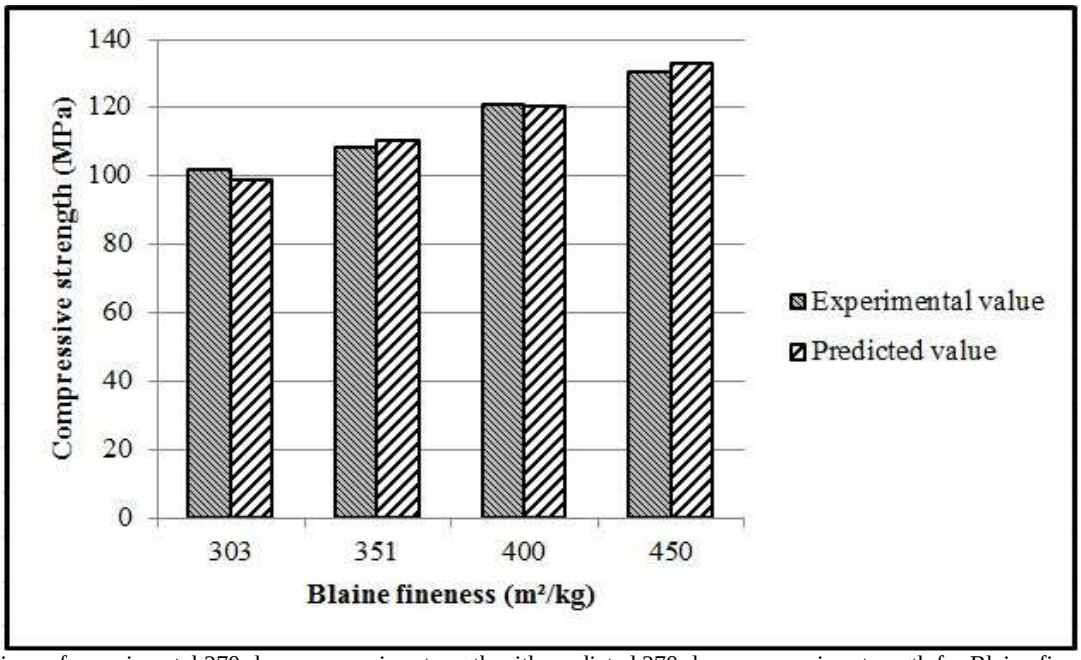


**Fig. 4** Comparison of experimental 270-day compressive strength with predicted 270-day compressive strength for Blaine finenesses of 303, 351, 400, and 450 $m^2/kg$

The average error (AE) values (%) are calculated by means of Eq. (7):

$$AE = \frac{1}{N}\sum_{1}^{N}\left|\frac{R_e - R_m}{R_e}\right| \times 100 \qquad (7)$$

In which $R_e$ and $R_m$ are experimental and model prediction of the compressive strength, respectively. AE values (%) of model at Blaine finenesses of 205, 250, 303, 351, 400, and 450 $m^2/kg$ are lower than 3, 2, 3, 3, 2, and 2, respectively. It can be concluded that the model is capable of predicting the compressive strength of CAPHSC mortar.

## 5. Conclusions

A mathematical model for prediction of the compressive strength of chemically activated high phosphorous slag content cement mortar has been proposed based on curve fitting and regression analysis. Input variables used in the model creation process included the curing time, water-to-cement ratio, and compressive strength. The obtained model is in logarithmic form and it has two parameters namely $\bar{\alpha}$ and $\bar{\beta}$. Parameter, $\bar{\beta}$, is only as a function of the water-to-cement ratio, while the parameter, $\bar{\alpha}$ is a constant value. The presented model is theoretically sound, easy to use and capable of predicting the compressive strength of chemically activated high phosphorous slag content cement at different Blaine finenesses and curing times. The average error of the model was no more than 3 percent.

## References

[1] Xia C, Li Z, Kunhe F. Anti-crack performance of phosphorous slag concrete, Wuhan University Journal of Natural Sciences, 2009, No. 1, Vol. 14, pp. 080-086.

[2] Xia C, Kunhe F, Huaquan Y, Hua P. Hydration kinetics of phosphorous slag-cement paste, Wuhan University Journal of Technology-Mater, 2011, No. 1, Vol. 26, pp. 142-146.

[3] Kumar S, Kumar R, Bandopadhyay A, Alex TC, Kumar BR, Das SK, Mehrotra SP. Mechanical activation of granulated blast furnace slag and its effect on the properties and structure of Portland slag cement, Cement & Concrete Composites, 2008, Vol. 30, pp. 679-685.

[4] Dong XL, Lin C, Zhong ZX, Zhi ML. A blended cement containing blast furnace slag and phosphorous slag, Journal of Wuhan University of Technology, 2002, No. 2, Vol. 17, pp. 62-65.

[5] Sajedi F, Razak HA. Comparison of different methods for activation of ordinary Portland cement-slag mortars, Construction and Building Materials, 2011, Vol. 25, pp. 30-38.

[6] Sajedi F, Razak HA. Effects of thermal and mechanical activation methods on compressive strength of ordinary Portland cement-salg mortar, Materials and Design, 2011, Vol. 32, pp. 984-995.

[7] Allahverdi A, Saffari M. Chemical activation of phosphorous slag with a solid compound activator, In: Proceedings of 4th International Conference on Non-Traditional Cements And Concretes 27-30 June, Brno, Czech Republic, 2011, pp. 573-580.

[8] Allahverdi A, Rahmani A. Chemical activation of natural pozzolan with a solid compound activator, Cement Wapno Beton, 2009, Vol. 4, pp. 205-213.

[9] Allahverdi A, Ghorbani J. Chemical activation and set acceleration of lime-natural pozzolan cement, Ceramic-Silikaty, 2006, Vol. 50, pp. 193-199.

[10] Dongxu L, Xuenquan W, Jinlin S, Yujiang W. The influence of compound admixtures on the properties of

high-content slag cement, Cement and Concrete Research, 2000, Vol. 30, pp. 45-50.

[11] Tsivilis S, Parissakis G. A mathematical-model for the prediction of cement strength, Cement and Concrete Research, 1995, Vol. 25, pp. 9-14.

[12] De Siquera Tango CE. An extrapolation method for compressive strength prediction of hydraulic cement products, Cement and Concrete Research, 1998, Vol. 28, pp. 969-983.

[13] Saridemir M. Prediction of compressive strength of concrete containing metakaolin and silica fume by artificial neural networks, Advances in Engineering Software, 2009, Vol. 40, pp. 350-355.

[14] Öztas A, Pala M, Özbay E, Kanca E, Caglar N, Bhatti MA. Prediction the compressive strength and slump of high strength concrete using neural network, Construction and Building Materials, 2006, Vol. 20, pp. 769-775.

[15] Bilim C, Atis CD, Tanyildizi H, Karahan O. Predicting the compressive strength of ground granulated blast furnace slag, Advances in Engineering Software, 2009, Vol. 40, pp. 334-340.

[16] Chen L. Grey and neural network prediction of concrete compressive strength using physical properties of electric arc furnace oxidizing slag, Journal of Environmental Engineering & Management, 2010, Vol. 20, pp. 189-194.

[17] Baykasoglu A, Dereli T, Tanis S. Prediction of cement strength using soft computing techniques, Cement and Concrete Research, 2004, Vol. 34, pp. 2083-2090.

[18] Iqbal khan M. Analytical model for the strength prediction of HPC consisting of cementitious composites, Architecture Civi Engineering Environment, 2009, Vol. 1, pp. 89-96.

[19] Chen L. A multiple linear regression prediction of concrete compressive strength based on physical properties of electric arc furnace oxidizing slag, International Joutnal of Applied Science and Engineering, 2010, Vol. 7, pp. 153-158.

[20] Eswari S, Raghunath PN, Kothandaraman S. Regression modeling for strength and toughness evaluation of hybrid fibre reinforced concrete, ARPN Journal of Engineering and Applied Sciences, 2011, Vol. 6, pp. 1819-6608.

[21] Deepa C, Sathiyakumari K, Sudha VP. Prediction of the compressive strength of high performance concrete mix using tree based modeling, International Journal of Computer Applications, 2010, Vol. 6, pp. 18-24.

[22] Dabic P, Krstulovic R, Rusic D. A new approach in mathematical modelling of cement hydration development, Cement and Concrete Research, 2000, Vol. 30, pp. 1017-1021.

[23] Lin F, Meyer C. Hydration kinetics modeling of Portland cement considering the effects of curing temperature and applied pressure, Cement and Concrete Research, 2009, Vol. 39, pp. 255-265.

[24] Zelic J, Rusic D, Krstulovic R. A mathematical model for prediction of compressive strength in cement-silica fume blends, Cement and Concrete Research, 2004, Vol. 34, pp. 2319-2328.

[25] Wong HS, Buenfeld NR. Determining the water-cement ratio, cement content, water content and degree of hydration of hardened cement paste: Method development and validation on paste samples, Cement and Concrete Research, 2009, Vol. 39, pp. 957-965.